Published in final edited form as:
Am J Ophthalmol. 2013 September ; 156(3): 578–587.e1. doi:10.1016/j.ajo.2013.04.015.

Estimated retinal ganglion cell counts in glaucomatous eyes with localized retinal nerve fiber layer defects

Andrew J. Tatham[1], **Robert N. Weinreb**[1], **Linda M. Zangwill**[1], **Jeffrey M. Liebmann**[2], **Christopher A. Girkin**[3], and **Felipe A. Medeiros**[1]

[1]Hamilton Glaucoma Center and Department of Ophthalmology, University of California, San Diego

[2]Department of Ophthalmology, New York Eye and Ear Infirmary, New York, New York

[3]Department of Ophthalmology, University of Alabama, Birmingham, Alabama

Abstract

Purpose—To estimate retinal ganglion cell (RGC) losses associated with visible glaucomatous localized retinal nerve fiber layer (RNFL) defects.

Design—Observational cross-sectional study.

Methods—A multicenter study of 198 normal eyes (138 subjects) and 66 glaucomatous eyes (55 subjects) recruited from the Diagnostic Innovations in Glaucoma Study and African Descent and Glaucoma Evaluation Study. All eyes had standard automated perimetry (SAP), spectral domain optical coherence tomography (SD-OCT) and fundus stereophotographs within 6 months. Glaucomatous eyes were included if localized RNFL defects were detected by masked grading of stereophotographs. The number of RGCs in each sector of a structure-function map was estimated using a previously published model combining RGC estimates from SAP and SD-OCT. The estimated percentage loss of RGCs (combined structure function index) was calculated.

Results—In glaucomatous eyes there were 136 sectors with visible RNFL defects and 524 sectors without visible RNFL defects. The commonest sectors with visible RNFL defects were inferior and inferotemporal sectors, followed by superior and superotemporal sectors. Eyes with visible RNFL defects had a mean estimated RGC count of 657,172 cells versus 968,883 cells in healthy eyes (P<0.001). The average combined structure function index in sectors with a visible RNFL defect (59±21%) was significantly higher than in sectors without a visible RNFL defect in glaucomatous eyes (15±29%, P<0.001) and higher than in healthy eyes (1±13%, P<0.001).

Corresponding Author: Felipe A. Medeiros, M.D., Ph.D. Hamilton Glaucoma Center University of California, San Diego 9500 Gilman Drive La Jolla, CA 92093-0946 fmedeiros@glaucoma.ucsd.edu Tel: 858-822-4592 Fax: 858-822-0615.

Financial Disclosure(s): Dr. Medeiros has a patent pending on the combined structure and function index. Drs Weinreb, Zangwill, Liebmann, Girkin, and Medeiros receive research support from Carl-Zeiss Meditec; Drs Weinreb, Zangwill, Liebmann, and Medeiros receive research support from Heidelberg Engineering; Dr Weinreb receives resource support from Optovue, Kowa, Nidek and Topcon; and Dr Weinreb is a consultant to Carl-Zeiss Meditec, Inc. and Topcon.

Contributions to Authors: Involved in Design and conduct of study (A.J.T., R.N.W., L.M.Z., J.M.L., C.A.G., F.A.M.); Collection, management, analysis, and interpretation of data (A.J.T., R.N.W., L.M.Z., J.M.L., C.A.G., F.A.M.); and Preparation, review, or approval of manuscript (A.J.T., R.N.W., L.M.Z., J.M.L., C.A.G., F.A.M.).

Registration information is available at the National Institute of Health database at http://www.clinicaltrials.gov. (Clinical trials identifiers: NCT00221923 and NCT00221897, September 14, 2005).

Conclusions—Although visible localized RNFL defects are often considered an early sign of glaucoma this study indicates that they are likely to be associated with large neuronal losses.

The histological hallmark of glaucoma is accelerated loss of retinal ganglion cells (RGCs) and RGC axons.[1-3] Loss of RGCs results in thinning of the retinal nerve fiber layer (RNFL),[4-6] topographical changes to the optic nerve head[1] and a reduction in visual field sensitivity, which can ultimately result in visual impairment and blindness.[6,7] Glaucomatous damage to the optic nerve head and RNFL can be quantified using methods such as confocal scanning laser ophthalmoscopy, scanning laser polarimetry[8] and optical coherence tomography (OCT).[9-14] RNFL loss can also be observed directly by dilated fundus examination using slit lamp biomicroscopy and an accessary biconvex non-contact hand-held lens.[15] In healthy eyes the RNFL has a bright, uniform striated appearance, and is most readily identifiable where the RNFL is thickest, close to the superior and inferior poles of the optic disc.[5] The RNFL striations represent bundles of RGC axons separated by Muller cell processes. The bright component of a striation is due to the highly reflective parallel RGC axon bundles and the dark bands between are due to the thick non-reflective dividing Muller cell glial septa.[16]

Loss of RGC axons leads to a reduction in the reflectivity of RGC axon bundles and may be diffuse or localized.[17,18] Diffuse axonal loss results in a general reduction in RNFL striations, a darkened appearance to the inner retina and increased visibility of the retinal blood vessels, which are normally embedded in the RNFL.[5,16,18] There is some evidence that localized loss is less common but more easily visible as it has sharply demarcated borders.[15,19] Localized RNFL defects tend to be wedge-shaped and narrower as the RNFL bundles converge towards the disc margin.[20] Although localized RNFL defects are occasionally caused by non-glaucomatous optic neuropathies, optic disc drusen, papilledema, or ischemic retinopathies, they have a high specificity for glaucoma and are not found in healthy eyes.[20-22] It has been proposed that localized RNFL defects may be the earliest observable clinical sign of glaucomatous damage.[7,17] However, a previous primate histological study found that a localized RNFL defect was only apparent on fundus photographs if more than 50% of the thickness of the RNFL had been lost.[4] Similar findings were found in another histological study of primate and human eyes, in which, localized loss of 28 to 45% of RNFL thickness was required for visible RNFL defects.[5] This suggests that rather than being an early sign of glaucoma a large number of RGCs are likely to have been lost before a visible RNFL defect develops.

Although direct quantification of RGCs *in vivo* is not yet possible, empirical formulas derived from clinical structural and functional tests may be used to estimate the number of RGCs. Estimates derived using these formulas have shown good correlation with histologic RGC counts in experimental glaucoma models.[6] In recent studies, we proposed a method for estimating RGC loss from a combination of standard automated perimetry (SAP) and RNFL assessment using OCT.[23-25] The combined structure function index (CSFI) was devised to represent the percentage of RGCs that an eye has lost compared to the expected number of RGCs. The combined structure function index performed significantly better than isolated structural and functional parameters for staging the disease and monitoring glaucomatous progression.[23] The estimated number of RGCs and the combined structure function index may also be calculated for individual regions of the optic nerve and retina using a structure-function map that relates the location of RGC soma to the position of RGC axons at the optic disc. The aim of this study was to estimate the quantity of RGCs lost in regions associated with localized RNFL defects visible on stereophotographs. RGC estimates in sectors with an RNFL defect were compared to RGC estimates in sectors without an RNFL defect and to estimates in healthy eyes.

Methods

This was an observational cross-sectional study involving participants from two prospective longitudinal studies; the African Descent and Glaucoma Evaluation Study (ADAGES) and the Diagnostic Innovations in Glaucoma Study (DIGS). The 3-site ADAGES collaboration includes the Hamilton Glaucoma Center at the Department of Ophthalmology, University of California, San Diego (UCSD) (data coordinating center); the New York Eye and Ear Infirmary; and the Department of Ophthalmology, University of Alabama, Birmingham. The DIGS includes only patients recruited at UCSD and the protocol is identical to that of the ADAGES. Methodological details have been described previously.[26] Informed consent was obtained from all the participants, and the institutional review boards and human subjects committees of all 3 sites prospectively approved all of the methods. All methods adhered to the tenets of the Declaration of Helsinki for research involving human subjects and the study was conducted in accordance with Health Insurance Portability and Accountability Act regulations.

The study included 66 eyes of 55 subjects with glaucoma and localized RNFL defects visible on fundus stereophotographs and 198 eyes of 138 healthy subjects. Healthy subjects were recruited from the general population and had intraocular pressure (IOP) of ≤21 mmHg or less with no history of raised IOP and normal SAP. At each visit, subjects underwent a comprehensive ophthalmologic examination including review of medical history, visual acuity, slit-lamp biomicroscopy, IOP measurement, gonioscopy, dilated fundoscopic examination, stereoscopic optic disc photography, Spectralis spectral domain OCT (SD-OCT) (Heidelberg Engineering, Dossenheim, Germany), and SAP using the Swedish interactive threshold algorithm (SITA Standard 24-2, Carl Zeiss Meditec, Inc., Dublin, CA, USA). Only subjects with open angles on gonioscopy were included. Subjects were excluded if they presented with a best-corrected visual acuity of less than 20/40, spherical refraction outside ±5.0 diopters and/or cylinder correction outside 3.0 diopters, or any other ocular or systemic disease that could affect the optic nerve or the visual field.

Stereophotograph Grading

All patients underwent simultaneous stereoscopic optic disc photography. Digital stereoscopic images were reviewed with a stereoscopic viewer (Screen-VU stereoscope, PS Mfg., Portland, Oregon, USA) by two or more experienced graders. Each grader was masked to the subject's identity and to the other test results. Details of the methodology employed to grade optic disc photographs at the UCSD Optic Disc Reading Center have been provided elsewhere.[26-28] Eyes with localized RNFL defects were identified by at least 2 graders to be included in this analysis. RNFL defects were defined as defects wider than twice the width of an arteriole, extending from close to the disc margin into the parapapillary area, widening en route (i.e., wedge-shaped).[20] Slit defects narrower than the diameter of adjacent vessels were not included as they are frequently found in normal eyes.[5,29]

Imaging and Standard Automated Perimetry

The Spectralis SD-OCT (software version 5.4.7.0, Heidelberg Engineering, Dossenheim, Germany) was used to obtain RNFL thickness measurements. The device uses a dual-beam SD-OCT and a confocal laser-scanning ophthalmoscope that works by emitting a superluminescent diode light with a center wavelength of 870 nm and an infrared scan to simultaneously provide images of ocular microstructures. A real-time eye tracking system is incorporated that couples confocal laser scanning ophthalmoscope and SD-OCT scanners to adjust for eye movements and to ensure that the same location of the retina is scanned over time. 1536 A-scan points were acquired from a 3.45-mm circle centered on the optic disc.

All images were reviewed by the UCSD Imaging Data Evaluation and Analysis Center to ensure the scan was centered, that the signal strength was >15dB and that there were no artifacts. Scans that were inverted, clipped or those that had coexistent retinal pathological abnormalities were excluded. The RNFL segmentation algorithm was also checked for errors.

All the patients underwent SAP testing using the SITA Standard 24-2 strategy less than 6 months apart from imaging. All visual fields were evaluated by the UCSD Visual Field Assessment Center.[30] Visual fields with more than 33% fixation losses or false-negative errors, or more than 15% false-positive errors, were excluded. An abnormal SAP result was defined as having a pattern standard deviation outside the 95% confidence limits or a glaucoma hemifield test result outside the reference range.

Data regarding optic disc area was collected using the Heidelberg Retina Tomograph (HRT) II (Heidelberg Engineering, Carlsbad, CA, USA).[27]

Estimation of retinal ganglion cell number

The estimates of RGC counts were obtained according to the model developed by Medeiros et al[23-25] based on empirical formulas derived by Harwerth et al[6] for estimating RGC counts from SAP and OCT. The details of the model and the empirical formulas used to derive RGC counts have been described in detail in previous publications.[23-25] The initial step of the model consists of translating SAP sensitivity values into RGC counts using formulas derived from experimental research in monkeys and subsequently translated to human eyes. The following formulas were used to estimate the number of RGC somas in retinal areas corresponding to specific SAP test field locations at eccentricity *ec* with sensitivity *s* in dB:

$$m=[0.054*(ec*1.32)]+0.9$$
$$b=[-1.5*(ec*1.32)]-14.8$$
$$gc=\{[(s-1)-b]/m\}+4.7$$
$$\text{sector } SAPrgc=\sum 10\hat{}(gc*0.1)$$

In the above formulas, *m* and *b* represent the slope and intercept, respectively, of the linear function relating ganglion cell quantity (*gc*) in dB to visual field sensitivity (*s*) in dB at a given eccentricity. A structure function map[6] was used to assign SAP test locations to 10 equal 36° sectors of the optic nerv e head RNFL circle scan. Figure 1 shows the structure function map for a right eye with sector 9 corresponding to the inferotemporal region of the optic disc. In the left eye structure function map, sector 9 also corresponds to the inferotemporal sector of the optic disc but numbering is counterclockwise. RGC estimates for individual SAP test locations were summed to estimate the number of RGC soma corresponding to each region of the optic disc.

The structural part of the model involved estimating the number of RGC axons from SD-OCT RNFL thickness measurements. The model took into account the effect of aging on axonal density and the effect of disease severity on the relationship between the neuronal and non-neuronal components of the RNFL. The structure function map had 10 sectors and therefore data from the commercially available 6 sector RNFL thickness map was not used. Instead, mean RNFL thickness in each of the 10 disc sectors of the structure function map was calculated from the 1,536 A-scan points of the 3.45mm SD-OCT circle scan (data from 154 adjacent A-scans were averaged for each of sectors 1 to 6 and data from 153 adjacent A-scans were averaged for sectors 7 to 10). The number of RGC axons at each sector of the optic nerve was estimated using the following formulas.

$$d=(-0.007*age)+1.4$$
$$c=(-0.26*sMD)+0.12$$
$$\text{sector } OCTrgc=10\hat{}(\{[\log 10(\text{sector RNFL}*10870*d)]*10-c\}*0.1)$$

In the above formulas, d is the axonal density (axons/μm^2), c is a correction factor for the severity of disease to take into account remodeling of RNFL axonal and non-axonal composition and *sMD* is the sector mean deviation. The *sMD* was calculated by measuring the deviation of the SAP sensitivity from the expected sensitivity of SAP test locations in each sector.[5] The expected values were derived from the SITA normative database using the method described by Harwerth and colleagues (Table 1).[6] The total SD-OCT derived RGC estimate was calculated as the sum of *OCTrgc* in all ten sectors. The estimates of RGC count obtained from SAP and SD-OCT were then averaged, with a previously described weighting according to the overall severity of disease, to obtain a weighted RGC count (*wrgc*).[23,25]

$$\text{sector } wrgc=(1+sMD/30)*\text{sector OCT}rgc+(-sMD/30)*\text{sector SAP}rgc$$

The weights were chosen to reflect the inverse relationship of disease severity and SAP and SD-OCT estimates, along the scale of MD values from 0 to -30dB. The rationale for the use of a weighting system has been described.[25] Estimates of sector *wrgc* were summed to provide an overall *wrgc* estimate. A linear regression model was then used to relate *wrgc* estimates to age and optic disc area in healthy eyes and to develop a model to predict expected RGC numbers. A model was generated for each sector of the structure-function map using a development sample of 169 healthy eyes recruited from the general population. To avoid model overfitting none of the eyes in the development sample were included in the subsequent analysis. After calculating the expected number of RGCs in each sector for each eye, the sector combined structure function index (CSFI) was calculated as an estimate of the percentage of RGCs lost in each sector.

$$\text{Sector CSFI}=[(\text{expected number of RGCs in sector}-\text{sector}\,wrgc)/(\text{expected number of RGCs in sector})]*100$$

The global combined structure function index was calculated as the percentage of RGCs lost in the whole eye using the global *wrgc*. The location of the RNFL defect was determined by fitting a 10-segment circle, corresponding to the 10 zones of the structure function map, to the image of the optic disc (Figure 1). The circumference of the 10-segment circle was adjusted for best possible fit to the margin of the optic disc. The sectors corresponding to the localized RNFL defects were determined by visual inspection (A.J.T.). If an RNFL defect straddled two sectors it was deemed to involve both sectors.

Statistical Analysis

Descriptive statistics included mean and standard deviation for normally distributed variables, and median, first-quartile and third-quartile values for non-normally distributed variables. Student *t*-tests were used for group comparison for normally distributed variables and Wilcoxon rank-sum test for continuous non-normal variables. For categorical variables, X^2 tests or Fisher exact tests were used.

For glaucomatous eyes, the combined structure function index in sectors with localized RNFL defects was compared to the combined structure function index in sectors without RNFL defects. The combined structure function index in sectors with localized RNFL

defects was also compared to the combined structure function index in the healthy eyes. Clustering by participant and by eye was included in the calculations to account for correlations between eyes of the same subject and between sectors from the same eye. All statistical analyses were performed with commercially available software (STATA, version 12; StataCorp LP, College Station, TX, USA). The α level (type I error) was set at 0.05.

Results

The study included 264 eyes of 193 individuals. There were 198 eyes of 138 healthy subjects and 66 eyes of 55 subjects with localized RNFL defects visible on stereophotographs. 76 (39.4%) participants were of African ancestry, 113 (58.5%) of European ancestry and 4 (2.1%) of other racial background. Forty-nine eyes with localized RNFL defects had perimetric glaucoma, with a SAP defect present on 2 or more consecutive tests, and 17 eyes had a localized RNFL defect but no repeatable SAP defect. The demographic details and descriptive statistics are shown in Table 2.

56 eyes had a single RNFL defect and 10 eyes had RNFL defects at two discontiguous locations, resulting in a total of 76 RNFL defects. There were no eyes with localized RNFL defects at more than 2 discontiguous locations. Twenty-six contiguous RNFL defects (34.2%) involved 1 sector, 40 contiguous RNFL defects (52.6%) involved 2 sectors, and 10 contiguous RNFL defects (13.2%) involved 3 sectors. There were therefore a total of 136 sectors with and 524 sectors without localized RNFL defects in the glaucomatous eyes. The commonest sectors with localized RNFL defects were sector 9 (52 eyes, 78.8%), sector 8 (46 eyes, 69.7%), sector 2 (12 eyes, 18.2%), sector 3 (10 eyes, 15.2%), sector 10 (7 eyes, 10.6%) and sector 7 (6 eyes, 9.1%). Localized RNFL defects involved sector 1 in 2 eyes and sector 5 in just 1 eye. There were no localized RNFL defects in sectors 4 or 6.

Figure 2 shows the distribution of the combined structure function index in sectors with visible RNFL defects. In glaucomatous eyes, the combined structure function index in sectors with visible RNFL defects (59 ± 21%, range 20 to 100%) was significantly higher than in sectors without visible RNFL defects (15 ± 29%; P<0.001) (Table 3). This indicates an average estimated RGC loss of 59% in sectors with visible localized RNFL defects, compared to an average estimated loss of 15% in sectors without visible RNFL defects. The mean CSFI in healthy eyes was 1 ± 13%, which was significantly less than in sectors without visible RNFL defects in glaucomatous eyes (P<0.001). This suggests that there is significant diffuse loss of RGCs in glaucomatous eyes, even in sectors without visible RNFL defects. Eyes with localized RNFL defects also had lower mean deviation (P<0.001), RNFL thickness (P<0.001) and estimated RGC count (P<0.001) than healthy eyes (Table 2). The sector combined structure function indices in healthy eyes were significantly lower than in glaucomatous eyes (Table 2), with the exception of sector 6 (P =0.985); a sector in which there were no RNFL defects. Figure 3 shows a box plot showing lower quartile, median, upper quartile and minimum and maximum values of combined structure function index for all sectors of healthy eyes compared to the sector combined structure function index for sectors of glaucomatous eyes with localized RNFL defects and sectors of glaucomatous eyes without localized RNFL defects.

The superior sector with the greatest number of RNFL defects was sector 3. The mean estimated number of RGCs in sector 3 was 57,475 ± 20,186 (range 5,949 to 78,964) cells in eyes with a localized RNFL defect in this sector compared to 137,559 ± 33,080 (range 70,131 to 230,183) cells in sector 3 in healthy eyes (P <0.001). The mean combined structure function index in sector 3 was 61 ± 14% (range 46 to 96%) in eyes with a localized RNFL defect in this sector compared to -2 ± 22% (range -72 to 51%) in healthy eyes (P<0.001). The inferior sector with the greatest number of RNFL defects was sector 8. The

mean estimated number of RGCs in sector 8 was 65,965 ± 34,931 (range 1,272 to 133,074) cells in eyes with a localized RNFL defect in this sector compared to 158,096 ± 33,239 (range 78,085 to 259,719) cells in sector 8 in healthy eyes (P<0.001). The mean combined structure function index in sector 8 was 58 ± 22% (range 20 to 99%) in eyes with a localized RNFL defect in this sector compared to -1 ± 18% (range -49 to 43%) in healthy eyes (P <0.001).

Sectors with an RNFL defect had significantly higher combined structure function indices than the immediately adjacent sectors (P <0.001). The mean combined structure function index in sectors immediately clockwise and counterclockwise to the sector involving the edge of the RNFL defect was 22 ± 24%. In eyes with localized RNFL defects, the sector with maximum combined structure function index was sector 9 in 21 eyes (31.8%), sector 8 in 17 eyes (25.8%), sector 10 in 8 eyes (12.1%) and sector 3 in 8 eyes (12.1%) (Figure 4). The maximum combined structure function index was in sectors 1, 2 and 7 in 3 eyes each (4.6% each), sector 5 in 2 eyes (3.0%) and sector 6 in 1 eye (1.5%). The mean combined structure function index in the sector with the maximum combined structure function index was 66 ± 21%. The sector with the maximum estimated RGC loss was in the same sector as a localized RNFL defect in 50 eyes (75.8%) and in the same or adjacent sector as a localized RNFL defect in 59 eyes (89.4%). Examples of eyes with localized RNFL defects are shown in Figures 5 and 6.

Discussion

This study demonstrates that localized RNFL defects visible on stereophotographs are likely to be associated with loss of large numbers of RGCs. Sectors with a visible RNFL defect had an average estimated RGC loss of 59% (range of 20 to 100%) in the affected sector. This finding is in agreement with the results of histological studies that found focal RNFL defects are visible on fundus photographs in regions where 28 to 50% of the thickness of the RNFL had been lost.[4,5] Localized RNFL defects, therefore indicate substantial loss of RGCs.

Sectors with an RNFL defect had significantly greater estimated RGC losses than sectors without RNFL defects and sectors of healthy eyes. For example, the superior sector with most RNFL defects was sector 3 (superior temporal). Eyes with an RNFL defect in sector 3 had an estimated 80,000 fewer cells in the involved sector than healthy eyes, representing an estimated RGC loss of 58%. The inferior sector with most RNFL defects was sector 8 (inferior temporal). Eyes with an RNFL defect in sector 8 had an estimated 92,000 fewer cells, which was also 58% fewer than estimated in healthy eyes. Examples of eyes with localized RNFL defects and large estimated RGC losses is demonstrated in Figure 5 (Left and middle columns). The left eyes of two patients with visible inferotemporal RNFL defects are shown. The RNFL defects each involve two sectors with estimated RGC loss of 57 to 68% and 81 to 85%. The SD-OCT RNFL thickness maps show inferotemporal thinning and SAP shows superior visual field defects, consistent with the location of the visible RNFL defects.

Although most sectors with localized RNFL defects had large estimated RGC losses, 11 of 136 sectors with an RNFL defect (8.1%) had estimated losses of less than 30%, including a single sector with an estimated loss of 20%. In all but one case, RNFL defects associated with an estimated RGC loss of ≤30% also involved a neighboring sector with a greater estimated loss. An RNFL defect may have been visible in some sectors with a relatively low combined structure function index due to the imperfect nature of the structure function map. Also, localized RNFL defects, by definition, are areas of abnormality within areas of relatively preserved RNFL[15] and, therefore, the visibility of a localized RNFL defect

depends on the thickness and arrangement of the RNFL in neighboring regions. Most RNFL defects were in the inferotemporal followed by the superotemporal regions. These regions are prone to glaucomatous damage but also RNFL defects in these zones are easier to detect because the RNFL is thicker.[16-18,29,31]Figure 5 also shows an example of an eye with an RNFL defect and relatively low estimated RGC losses (Right column). In this case, the sectors corresponding to the visible RNFL defect had combined structure function indices of 21 and 35%; however, the adjacent sectors had estimated RGC losses of only 0 and 5%. The RNFL defect may be visible in this eye because of relative preservation of RGCs in adjacent sectors.

In contrast, some sectors had no visible RNFL defect despite high estimated RGC losses. Previous studies have shown that eyes with advanced glaucoma are less likely to have localized RNFL defects visible on stereophotographs as defects broaden and become diffuse with disease progression. [1,7,20,32] Therefore, there is no longer an area of abnormality within an area of relatively preserved RNFL. Visibility of RNFL defects also depends on age, race and disease severity.[1,7,15,20] The RNFL is easier to discern in younger subjects and therefore focal defects may be more easily detected. Eyes of younger patients also have greater RGC counts. However, there was no significant difference in the age of subjects with glaucoma and healthy participants. In this study there was a higher proportion of African-Americans in the group with RNFL defects than the group with healthy eyes. This is likely to be because RNFL defects are more visible in eyes with more deeply pigmented retinal pigment epithelium and choroid.

Localized RNFL defects are considered one of the earliest changes of glaucoma.[7,17,32] In this study, 17 of 66 eyes with visible RNFL defects (25.8%) had no repeatable SAP defect, despite estimated global RGC losses of 25% ± 9%. Figure 6 shows an eye with an RNFL defect involving two inferior sectors but with SAP indices within statistically normal limits. Despite the normal SAP indices, the combined structure function index indicates an estimated RGC loss of almost 50% in sectors corresponding to the visible RNFL defect. These results indicate that RNFL defects may be associated with large RGC losses even in eyes with normal visual fields. The spatial relationship between localized RNFL defects and the sector of maximal estimated RGC loss was also examined. The localized RNFL defects were in the same or adjacent sector as the sector with the maximum combined structure function index in almost 90% of eyes. This suggests good correlation between the RGC estimates and the stereoscopic photographs. There are, however, limitations to this comparison as the sector with maximum RGC loss may be different from the sector with an RNFL defect, for example, in an eye with advanced glaucoma and diffuse damage in one hemifield and an RNFL defect in the other hemifield. Discordance between the location of maximum estimated RGC loss and an RNFL defect may also have been due to individual anatomic variations or due to rotation of the OCT or disc photo during image acquisition. Efforts were taken to minimize rotation errors and ensure correct alignment during image acquisition. The Spectralis SD-OCT also has a fovea-to-disc (FoDi) alignment technology, which was used to automatically track and anatomically align circle scans and help overcome measurement errors due to changing head or eye position during scanning.

Other limitations of this study include the use of empirically derived formulas to estimate the number of RGCs. The original formulas were derived from studies in a primate model of glaucoma[6] and were developed from studies using time domain OCT. Despite these limitations, the formulas have been validated in multiple external human cohorts, including using SD-OCT.[23-25] There may have been eyes where localized RNFL defects were not detected, however; efforts were made to minimize errors by using two masked graders. RNFL defects may have been detected in more eyes and their borders may have been better delineated if we had used a different method of photographic acquisition, for example, a red-

free source of illumination. Red-free light is absorbed by melanin in the RPE and choroid and therefore creates a dark background in contrast to the white striations of the RNFL.[15] A computerized method of RNFL defect detection might also have identified localized RNFL defects in other eyes.[33] We decided to use plain light stereophotographs as this reflects a commonly used method of clinical assessment.

In conclusion, this study indicates that eyes with localized RNFL defects visible on stereophotographs are likely to have, on average, 39% fewer RGCs than a healthy eye of similar age subject. Localized RGC loss in the region of the RNFL defect is likely to be particularly high, as the sector corresponding to the RNFL defect had on average 59% fewer RGCs than expected. Therefore, rather than being an early sign of glaucoma, localized RNFL defects visible on stereophotographs and with slit lamp biomicroscopy are likely to be associated with large neuronal losses. The results suggest that sectorial analysis using the combined structure function index is a useful method to identify areas of localized RNFL loss and glaucomatous damage.

Acknowledgments

Funding Support: Supported in part by National Institutes of Health/National Eye Institute grants EY021818 (F.A.M.),EY11008 (L.M.Z.), EY14267 (L.M.Z.), EY019869 (L.M.Z.); an unrestricted grant from Research to Prevent Blindness (New York, NY); grants for participants' glaucoma medications from Alcon, Allergan, Pfizer, Merck and Santen.

References

1. Quigley HA, Green WR. The histology of human glaucoma cupping and optic nerve damage: clinicopathologic correlation in 21 eyes. Ophthalmology. 1979; 86(10):1803–1830. [PubMed: 553256]
2. Blumenthal EZ, Weinreb RN. Assessment of the retinal nerve fiber layer in clinical trials of glaucoma neuroprotection. Surv Ophthalmol. 2001; 45(3):S305–12. discussion S332-4. [PubMed: 11377454]
3. Kerrigan-Baumrind LA, Quigley HA, Pease ME, Kerrigan DF, Mitchell RS. Number of ganglion cells in glaucoma eyes compared with threshold visual field tests in the same persons. Invest Ophthalmol Vis Sci. 2000; 41(3):741–748. [PubMed: 10711689]
4. Quigley HA, Addicks EM. Quantitative studies of retinal nerve fiber layer defects. Arch Ophthalmol. 1982; 100(5):807–814. [PubMed: 7082210]
5. Quigley HA. Examination of the retinal nerve fiber layer in the recognition of early glaucoma damage. Trans Am Ophthalmol Soc. 1986; 84:920–66. [PubMed: 3109098]
6. Harwerth RS, Wheat JL, Fredette MJ, Anderson DR. Linking structure and function in glaucoma. Prog Retin Eye Res. 2010; 29(4):249–271. [PubMed: 20226873]
7. Sommer A, Katz J, Quigley HA, et al. Clinically detectable nerve fiber atrophy precedes the onset of glaucomatous field loss. Arch Ophthalmol. 1991; 109(1):77–83. [PubMed: 1987954]
8. Medeiros FA, Zangwill LM, Bowd C, Mohammadi K, Weinreb RN. Comparison of scanning laser polarimetry using variable corneal compensation and retinal nerve fiber layer photography for detection of glaucoma. Arch Ophthalmol. 2004; 122(5):698–704. [PubMed: 15136317]
9. Lee EJ, Kim TW, Weinreb RN, Park KH, Kim SH, Kim DH. Trend-based analysis of retinal nerve fiber layer thickness measured by optical coherence tomography in eyes with localized nerve fiber layer defects. Invest Ophthalmol Vis Sci. 2011; 52(2):1138–1144. [PubMed: 21051691]
10. Leung CK, Yu M, Weinreb RN, Lai G, Xu G, Lam DS. Retinal nerve fiber layer imaging with spectral-domain optical coherence tomography: patterns of retinal nerve fiber layer progression. Ophthalmology. 2012; 119(9):1858–1866. [PubMed: 22677426]
11. Kim TW, Park UC, Park KH, Kim DH. Ability of Stratus OCT to identify localized retinal nerve fiber layer defects in patients with normal standard automated perimetry results. Invest Ophthalmol Vis Sci. 2007; 48(4):1635–1641. [PubMed: 17389494]

12. Lu AT, Wang M, Varma R, et al. Combining nerve fiber layer parameters to optimize glaucoma diagnosis with optical coherence tomography. Ophthalmology. 2008; 115(8):1352–1357. [PubMed: 18514318]
13. Weinreb RN. Laser scanning tomography to diagnose and monitor glaucoma. Curr Opin Ophthalmol. 1993; 4(2):3–6. [PubMed: 10148455]
14. Jeoung JW, Park KH, Kim TW, Khwarg SI, Kim DH. Diagnostic ability of optical coherence tomography with a normative database to detect localized retinal nerve fiber layer defects. Ophthalmology. 2005; 112(12):2157–2163. [PubMed: 16290196]
15. Quigley HA, Sommer A. How to use nerve fiber layer examination in the management of glaucoma. Trans Am Ophthalmol Soc. 1987; 85:254–272. [PubMed: 3447335]
16. Radius RL, Anderson DR. The histology of retinal nerve fiber layer bundles and bundle defects. Arch Ophthalmol. 1979; 97(5):948–950. [PubMed: 109068]
17. Hoyt WF, Schlicke B, Eckelhoff RJ. Fundoscopic appearance of a nerve-fibre-bundle defect. Br J Ophthalmol. 1972; 56(8):577–583. [PubMed: 5079403]
18. Airaksinen PJ, Drance SM, Douglas GR, Mawson DK, Nieminen H. Diffuse and localized nerve fiber loss in glaucoma. Am J Ophthalmol. 1984; 98(5):566–571. [PubMed: 6496612]
19. Tuulonen A, Airaksinen PJ. Initial glaucomatous optic disk and retinal nerve fiber layer abnormalities and their progression. Am J Ophthalmol. 1991; 111(4):485–490. [PubMed: 2012151]
20. Jonas JB, Schiro D. Localized retinal nerve fiber layer defects in nonglaucomatous optic nerve atrophy. Graefes Arch Clin Exp Ophthalmol. 1994; 232(12):759–760. [PubMed: 7890191]
21. Jonas JB, Schiro D. Localised wedge shaped defects of the retinal nerve fibre layer in glaucoma. Br J Ophthalmol. 1994; 78(4):285–290. [PubMed: 8199115]
22. Quigley HA, Reacher M, Katz J, Strahlman E, Gilbert D, Scott R. Quantitative grading of nerve fiber layer photographs. Ophthalmology. 1993; 100(12):1800–1807. [PubMed: 8259277]
23. Medeiros FA, Lisboa R, Weinreb RN, Girkin CA, Liebmann JM, Zangwill LM. A combined index of structure and function for staging glaucomatous damage. Arch Ophthalmol. 2012; 130(9):1107–1116. [PubMed: 23130365]
24. Medeiros FA, Zangwill LM, Anderson DR, et al. Estimating the rate of retinal ganglion cell loss in glaucoma. Am J Ophthalmol. 2012; 154(5):814–824. [PubMed: 22840484]
25. Medeiros FA, Zangwill LM, Bowd C, Mansouri K, Weinreb RN. The Structure and Function Relationship in Glaucoma: Implications for Detection of Progression and Measurement of Rates of Change. Invest Ophthalmol Vis Sci. 2012; 53(11):6939–6946. [PubMed: 22893677]
26. Sample PA, Girkin CA, Zangwill LM, et al. The African Descent and Glaucoma Evaluation Study (ADAGES): design and baseline data. Arch Ophthalmol. 2009; 127(9):1136–1145. [PubMed: 19752422]
27. Medeiros FA, Vizzeri G, Zangwill LM, Alencar LM, Sample PA, Weinreb RN. Comparison of retinal nerve fiber layer and optic disc imaging for diagnosing glaucoma in patients suspected of having the disease. Ophthalmology. 2008; 115(8):1340–1346. [PubMed: 18207246]
28. Medeiros FA, Weinreb RN, Sample PA, et al. Validation of a predictive model to estimate the risk of conversion from ocular hypertension to glaucoma. Arch Ophthalmol. 2005; 123(10):1351–1360. [PubMed: 16219726]
29. Leung CK, Choi N, Weinreb RN, et al. Retinal nerve fiber layer imaging with spectral-domain optical coherence tomography: pattern of RNFL defects in glaucoma. Ophthalmology. 2010; 117(12):2337–2344. [PubMed: 20678802]
30. Racette L, Liebmann JM, Girkin CA, et al. African Descent and Glaucoma Evaluation Study (ADAGES): III. Ancestry differences in visual function in healthy eyes. Arch Ophthalmol. 2010; 128(5):551–559. [PubMed: 20457975]
31. Jonas JB, Nguyen NX, Naumann GO. The retinal nerve fiber layer in normal eyes. Ophthalmology. 1989; 96(5):627–632. [PubMed: 2748120]
32. Sommer A, Miller NR, Pollack I, Maumenee AE, George T. The nerve fiber layer in the diagnosis of glaucoma. Arch Ophthalmol. 1977; 95(12):2149–2156. [PubMed: 588106]

33. Muramatsu C, Hayashi Y, Sawada A, et al. Detection of retinal nerve fiber layer defects on retinal fundus images for early diagnosis of glaucoma. J Biomed Opt. 2010; 15(1):016021. [PubMed: 20210467]

Andrew Tatham Biosketch

Andrew J. Tatham is Visiting Glaucoma Fellow at the Hamilton Glaucoma Center, University of California, San Diego. He undertook resident and glaucoma fellowship training at University Hospitals Leicester and Moorfields Eye Hospital, United Kingdom. He has achieved several prizes including the Pfizer Ophthalmic Fellowship from the Royal College of Ophthalmologists and the award for highest score at the European Board of Ophthalmology examinations. His research interests are glaucoma imaging and structure-function relationships in glaucoma.

Figure 1.
Illustration of the structure function map for the right eye used for sectorial estimation of retinal ganglion cell counts. The map divides the standard automated perimetry plot into 10 sectors (Left), with 10 corresponding optic disc sectors, each of 36-degrees.(Center) The location of the retinal nerve fiber layer defect was determined by fitting a 10-segment circle, corresponding to the 10 zones of the structure function map, to the optic disc photograph. (Right) In this example, the visible nerve fiber defect is in sector 8.

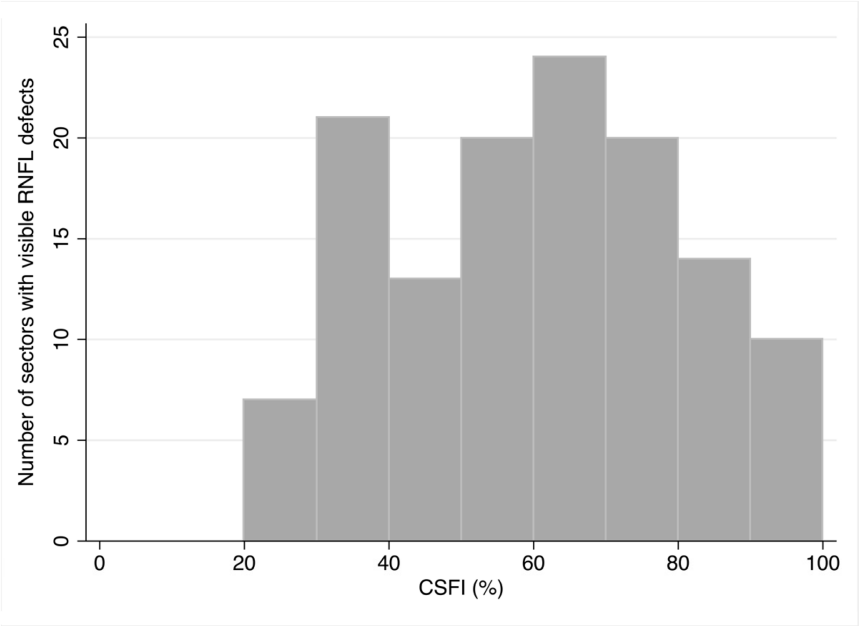

Figure 2.
Histogram showing the distribution of estimated retinal ganglion cell loss (estimated using the combined structure function index (CSFI)) in sectors of glaucomatous eyes with visible localized retinal nerve fiber layer (RNFL) defects.

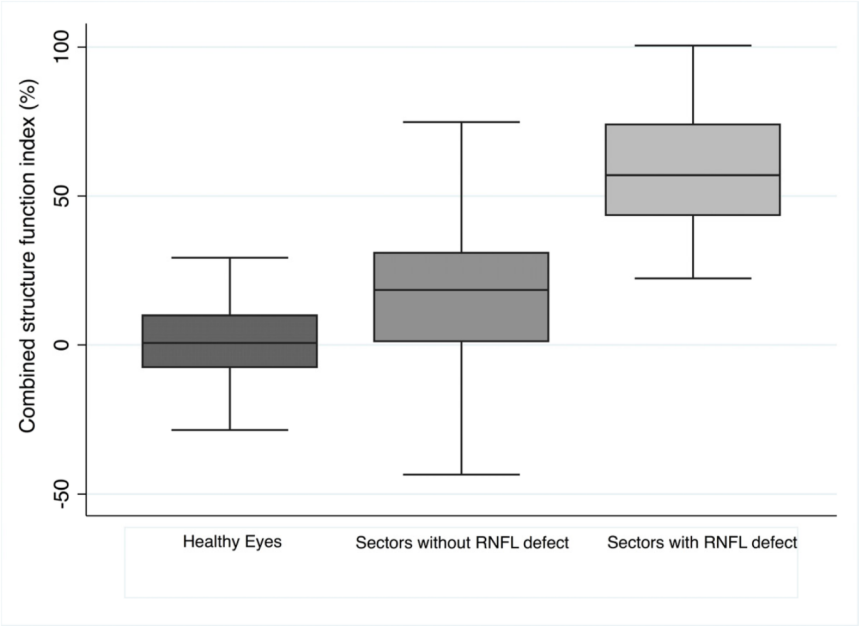

Figure 3.

Box plot showing the distribution of estimated retinal ganglion cell loss (estimated using the combined structure function index (CSFI)) in all sectors of healthy eyes compared to the combined structure function index in sectors with visible localized retinal nerve fiber layer (RNFL) defects and the combined structure function index in sectors of glaucomatous eyes without visible localized RNFL defects.

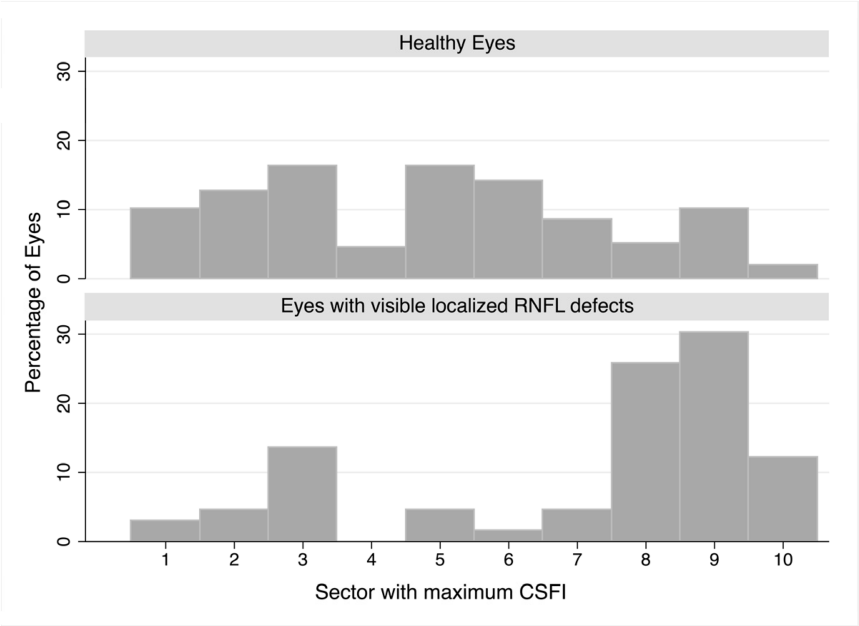

Figure 4.

Histogram showing the distribution of sectors with the greatest estimated retinal ganglion cell loss (estimated using the combined structure function index (CSFI)) for healthy eyes (Top) and glaucomatous eyes with a visible localized retinal nerve fiber (RNFL) defect. (Bottom)

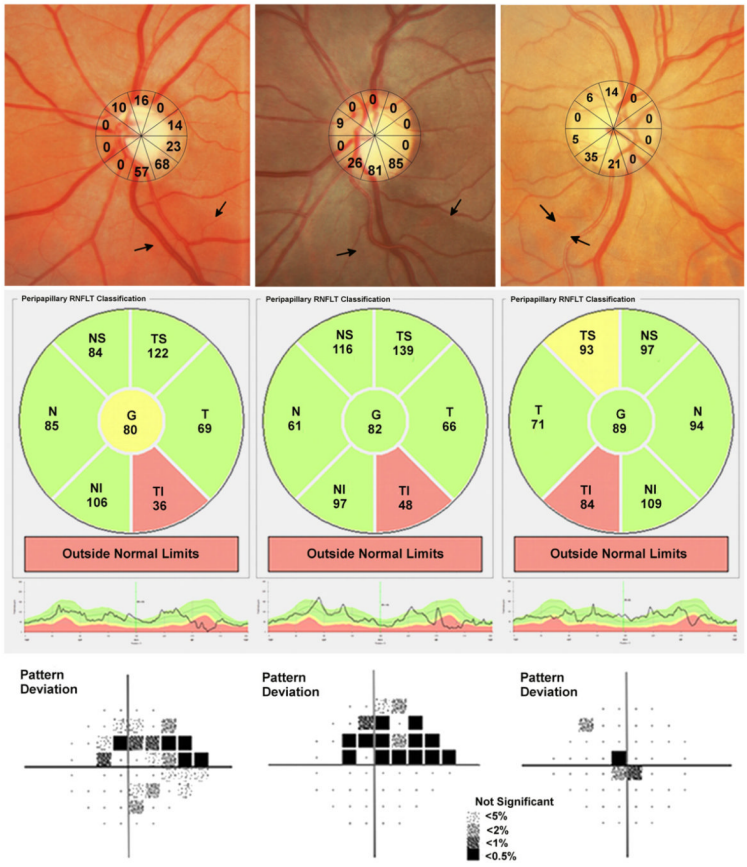

Figure 5.

Examples of 3 glaucomatous eyes with visible localized retinal nerve fiber layer (RNFL) defects. The optic disc photographs show the estimated retinal ganglion cell loss (estimated using the combined structure function index) in each of ten sectors of the structure function map.(Top row) The first example shows a visible RNFL defect inferior-temporal to the optic disc.(Top left) The estimated retinal ganglion cell loss in the two sectors corresponding to the defect is 57 to 68%. There is good agreement with the spectral domain optical coherence tomography RNFL thickness map, which shows RNFL loss in the inferior-temporal region (Center left) and with standard automated perimetry showing a superior arcuate defect. (Bottom left). The second example shows a RNFL defect associated with an estimated retinal ganglion cell loss of 81 to 85% (Top center) and the third example a RNFL defect associated with an estimated retinal ganglion cell loss of 21 to 35%.(Top right) The corresponding spectral domain optical coherence tomography (Center row) and standard automated perimetry (Bottom row) results for these eyes are also shown.

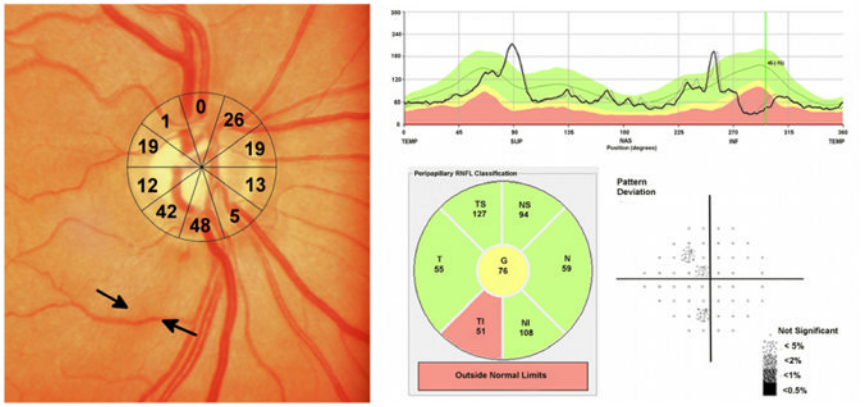

Figure 6.

Example of an eye of a 70 year-old subject with a localized retinal nerve fiber (RNFL) defect visible on optic disc photography.(Left) The RNFL defect corresponded to two sectors of the structure function map with an estimated retinal ganglion cell loss of 42 to 48%.(Left) The estimated retinal ganglion cell loss in the other sectors is also shown.(Left) Spectral domain optical coherence tomography revealed localized thinning of the RNFL in the inferior-temporal region.(Top right and Bottom center) Despite high estimated retinal ganglion cell losses, standard automated perimetry global indices were within statistically normal limits.(Bottom right)

Tabel 1

Predicted mean visual field sensitivities for healthy eyes in each of the 10 sectors of the structure function map used for sectorial estimation of retinal ganglion cell numbers.

Sector Number	1	2	3	4	5	6	7	8	9	10
Slope (dB/year)	-0.057	-0.061	-0.060	-0.062	-0.057	-0.057	-0.061	-0.057	-0.062	-0.060
Intercept (dB)	34.68	33.60	33.32	31.68	31.68	31.68	31.19	33.46	33.01	34.45

Am J Ophthalmol. Author manuscript; available in PMC 2014 September 01.

Tabel 2

Comparison of demographic information, mean deviation on standard automated perimetry, mean retinal nerve fiber layer thickness, and estimated retinal ganglion cell losses (estimated using the combined structure function index) for healthy and glaucomatous subjects (those with visible localized retinal nerve fiber layer defects) (n = 193 subjects, 264 eyes).

	Healthy Eyes = 198 Subjects = 138	**Visible localized RNFL defect Eyes = 66 Subjects = 55**	**P Value**
Age (years)[a]	62.5 (55.7 to 69.5)	63.4 (56.1 to 71.6)	0.248[c]
Race			0.001[d]
White = 0	0 = 126	0 = 27	
Black = 1	1 = 72	1 = 39	
Mean Deviation (dB)	-0.1 (-1.0 to 1.0)	-3.3 (-5.9 to -1.4)	<0.001[c]
Mean RNFL thickness (um)	96.3 ± 10.2	76.0 ± 12.9	<0.001[b]
Estimated number of RGCs	968,883 ± 170,230	657,172 ± 163,599	<0.001[b]
Global CSFI (%)	1 ± 13	39 ± 15	<0.001[b]
CSFI1 (%)	4 ± 19	10 ± 27	0.027[b]
CSFI2 (%)	1 ± 21	13 ± 31	0.007[b]
CSFI3 (%)	-2 ± 22	30 ± 22	<0.001[b]
CSFI4 (%)	-1 ± 20	19 ± 23	<0.001[b]
CSFI5 (%)	2 ± 28	16 ± 30	0.012[b]
CSFI6 (%)	3 ± 27	4 ± 34	0.985[b]
CSFI7 (%)	2 ± 23	26 ± 28	<0.001[b]
CSFI8 (%)	-1 ± 18	52 ± 24	<0.001[b]
CSFI9 (%)	2 ± 21	52 ± 26	<0.001[b]
CSFI10 (%)	3 ± 16	19 ± 42	0.004[b]

RNFL = retinal nerve fiber layer; dB = decibels; RGCs = retinal ganglion cells; CSFI = combined structure function index; CSFI1 to CSFI10 = combined structure function index in each sector (1 to 10) of the structure function map.

[a] Median (interquartile range)

[b] t-test

[c] Wilcoxon-Rank sum test

[d] Chi-square test

Tabel 3

Estimated (mean ± standard deviation) retinal ganglion cell losses (estimated using the combined structure function index) by sector for glaucomatous eyes for each of the ten sectors of a structure function map. Sectors with and without visible localized retinal nerve fiber layer defects are compared (n = 660 sectors).

	Number of RNFL defects	CSFI for sectors of glaucomatous eyes without RNFL defects	CSFI for sectors of glaucomatous eyes with RNFL defects	P values[a]
Sector 1	2	9 ± 27	43	
Sector 2	12	5 ± 27	50 ± 17	<0.001
Sector 3	10	25 ± 18	61 ± 14	<0.001
Sector 4	0	19 ± 23	No eyes with defect in sector 4	
Sector 5	1	16 ± 30	65	
Sector 6	0	4 ± 34	No eyes with defect in sector 6	
Sector 7	6	23 ± 27	62 ± 18	<0.001
Sector 8	46	39 ± 22	58 ± 22	0.002
Sector 9	52	23 ± 22	60 ± 20	<0.001
Sector 10	7	12 ± 38	75 ± 32	<0.001
All sectors	136	15 ± 29	59 ± 21	<0.001

RNFL = retinal nerve fiber layer; CSFI = combined structure function index.

[a] t test.